NON-CONFORMAL FINITE ELEMENT HOMOGENIZATION APPLIED TO WOVEN COMPOSITES WITH COMPLEX TEXTILE ARCHITECTURES

CONFERENCE PAPER · JULY 2015

7 AUTHORS, INCLUDING:


David Dumas
Cenaero
5 PUBLICATIONS **0** CITATIONS


Thomas Pardoen
Université catholique de Louvain
231 PUBLICATIONS **3,941** CITATIONS

Christian Bailly
Université catholique de Louvain
169 PUBLICATIONS **2,435** CITATIONS


Frédéric Lani
Université catholique de Louvain
39 PUBLICATIONS **363** CITATIONS

NON-CONFORMAL FINITE ELEMENT HOMOGENIZATION APPLIED TO WOVEN COMPOSITES WITH COMPLEX TEXTILE ARCHITECTURES

Benoît Wucher[1], Stefan Hallström[2], David Dumas[1], Thomas Pardoen[3], Christian Bailly[4], Philippe Martiny[5] and Frédéric Lani[3]

[1]Composite Structures and Processes, Cenaero ASBL
Rue des Frères Wright 29, B-6041 Gosselies, Belgium
Email: benoit.wucher@cenaero.be, web page: http://www.cenaero.be

[2]Dept. of Aeronautical and Vehicle Engineering, KTH Royal Institute of Technology
SE-100 44 Stockholm, Sweden
Email: stefanha@kth.se, web page: https://www.kth.se/en

[3]Institute of Mechanics, Materials and Civil Engineering, Université catholique de Louvain
Place Sainte Barbe 2, B-1348 Louvain-la-Neuve, Belgium
Email: thomas.pardoen@uclouvain.be, web page: http://www.uclouvain.be

[4]Institute of Condensed Matter and Nanosciences, Université catholique de Louvain
Croix du Sud 1, B-1348 Louvain-la-Neuve, Belgium
Email: christian.bailly@uclouvain.be, web page: http://www.uclouvain.be

[5]e-Xstream engineering, MSC Software
Rue Emile Francqui 9, B-1435 Mont-Saint-Guibert, Belgium
Email: philippe.martiny@e-xstream.com, web page: http://www.e-xstream.com

Keywords: Homogenization, Finite elements, Non-conformal mesh, 3D textiles

ABSTRACT

A simple finite element homogenization procedure is developed for application to fiber composites with complex woven reinforcement architectures, typically 3D textiles. The purpose of the method is to accurately evaluate properties of the composite using finite element methods, with limited modeling effort. The open-source software TexGen is used to model simplified versions of complex textiles, while keeping their main characteristics intact. This leads to high penetrations, which prevent conventional meshing. A non-conformal meshing procedure is adopted, where the mesh is refined at material interfaces. Penetrations are mitigated by correcting locally the material properties of the yarns to account for their correct fiber content. The method is also compared to more sophisticated textile modeling approaches.

1 INTRODUCTION

Homogenization of fiber reinforced polymers, and more specifically of textile composites, has received considerable attention in the last decades. It consists in modeling a representative volume element (RVE) of the presumably periodic textile architecture, and in using a homogenization scheme to determine the thermo-mechanical behavior of the RVE. Textile modeling and homogenization schemes constitute two separate lines of research, of which a brief and non-exhaustive review is presented here.

Analytical or semi-analytical schemes rely on the complementary variational principle, like the approach proposed by Vandeurzen et al. [1,2] or the generalized method of cells [3]. Mean-field techniques such as the Mori-Tanaka method are very efficient in predicting homogenized properties [4] but give access only to the mean stress and strain values within the RVE and not to their detailed distribution across the microstructure.

A more detailed description of the microstructure of the RVE can be generated through finite element (FE) based approaches. The present study focuses on such techniques. Classical approaches can either use explicit meshes of yarns and of the resin rich domains, or non-conformal meshes that do not align element edges with yarn boundaries (of which a typical example is voxel meshing). Although explicit meshes are the most reliable method for modeling detailed microscopic stress states inside the RVE, a recognized limitation of this approach is the need to introduce an artificial resin layer between the yarns [5,6]. This artificial layer can lead to an overestimation of the total thickness of the laminate [7]. Voxel approaches [8-15] describe the textile as a grid of uniformly-sized hexahedra. By essence, the irregularity of the yarn boundaries description leads to spurious stress concentrations but they are still widely used in linear elastic homogenization and in failure analysis [10,15] contexts, especially when conformal meshing becomes too complicated.

Textile modeling is the step preceding homogenization and is of equal importance. To this day, the WiseTex software package [5,16-18] and the Digimat tool suite [19,20] are probably the most complete homogenization solutions. WiseTex provides a framework to model a wide range of textiles with analytical [18] or FE tools [5] for permeability [17] or mechanical analysis. Digimat offers a range of capabilities to model not only textile composites but also short-fiber reinforced plastics and discontinuous fiber composites both with FE-based and semi-analytical methods. The TexGen software package [21] provides an efficient open-source alternative, but its capabilities are more limited. On the contrary, very fine modeling techniques were developed. One of the main purposes of refined textile modeling is to avoid penetrations, either during [6,9,22-24] or a posteriori [5,16,25,26] to the textile generation.

The present work investigates an alternative approach, where the main idea is not to avoid or suppress penetrations, but to ally simple geometrical modeling with the power and universality of classical FE analysis. To this end, textiles are modeled in the open-source software TexGen by keeping a few key parameters comparable to the real textile, such as fiber content, crimp or yarn paths. This approach leads to large penetrations for highly-compacted textiles. They prevent conventional meshing, and therefore a non-conformal mesh is used. In the intent of rationalizing the mesh size compared to classical hexahedral voxels, the mesh is unstructured and refined at the yarn/matrix interface. Penetrations are compensated by adapting locally the fiber volume fraction inside the yarns. The proposed methodology can be applied to any textile but is more relevant for the ones that are complex to represent geometrically, namely 3D woven textiles. While the framework is, in principle, not limited to linear elasticity, other considerations such as failure mechanisms are out of the scope of this paper, focusing on the method more than on its applications.

2 NON-CONFORMAL MESHING

The starting point of the present work is to perform homogenization FE analysis on penetrating textile models. The presented methodology is applied on 3D models (i.e. volume meshes), but it is explained in two dimensions for better clarity. Let us consider a penetrating textile such as in Figure 1, where two yarns are modeled by ellipses within a box representing the RVE. Due to the penetration, this RVE cannot be meshed by a conventional method, where the mesh would match the boundaries of the yarns. Therefore, a non-conformal meshing methodology is used. The most classical approach would be to use a uniformly-sized voxel mesh as in Figure 2a. This mesh has the disadvantages of being both over-refined in the resin region and not refined enough around the yarn boundaries. A technique to produce a voxel mesh refined at the yarn boundaries has been developed by Kim and Swan [14]. This method has an additional constraint in the sense that it provides a disconnected mesh. Therefore, cumbersome post-treatment needs to be applied in order to create suitable multi-point constraints (MPCs). Another approach is adopted here to rationalize the mesh size while keeping a normal connected mesh. An accurate non-conformal representation of the yarn boundaries is ensured through a mesh adaptation procedure. To this end, a signed distance field is computed as proposed by

Sonon and Massart [24]. As can be seen in Figure 3, this algorithm captures, in a very generic manner, the yarn boundaries as well as the separation between the two yarns when contouring the iso-zero of the distance field. The algorithm does not provide the Euclidian distance in penetration zones, but this has no impact on the proposed methodology. Then, MeshSim libraries from Simmetrix Inc. [27] are used for the mesh adaptation procedure which uses the distance field as an input to dictate the mesh size. The mesh size is defined as a piecewise-linear function of the distance to those boundaries, i.e.,

$$s(x,y,z) = \max(m, \min(M, 0.8 \times |\, d(x,y,z)|)), \tag{1}$$

where x, y, z are the space coordinates, s is the mesh size field, d is the signed distance field, and m and M are the user-defined minimum and maximum mesh sizes, respectively. The 0.8 factor comes from the fact that the code Simmetrix cannot increase the mesh size s as fast as the distance d increases. The mesh shown in Figure 2b is periodic on opposite faces, as necessary for homogenization purposes. This is ensured by mesh copying from one face to its opposite face, and by the fact that the distance field is made periodic by duplicating the textile geometry in all directions of periodicity. As illustrated in Figure 2, the signed distance field also leads to a classification of each element in the relevant entity (resin, yarn n°1 or yarn n°2) based on the position of its centroid, for the subsequent homogenization analysis. Both 2D meshes in Figure 2 are quadratic and have the same number of nodes, around 14,000. However, one can see that the yarn boundaries are much more accurately represented with the unstructured approach, compared to the voxel approach. In that sense, the number of degrees of freedom is rationalized by the present meshing procedure because the mesh is refined only where it needs to be. This fact is emphasized by the mesh sensitivity study performed on this example textile and presented in Figure 4. This graph shows the irregularity of the non-conformal yarn boundaries as a function of mesh refinement for both unstructured and structured (voxel) approaches. The interface irregularity I_{avg} is computed as the positive distance $|d(x,y,z)|$ averaged over all interface nodes, divided by the smallest dimension of the RVE. A node is an interface node if it belongs to an element crossed by the iso-zero of the distance field. Therefore, I_{avg} is an indicator of the smoothness of the separation between the yarns and the resin, and between the yarns themselves. The unstructured mesh has a clear advantage, with an average irregularity I_{avg} less than half that of the structured mesh when there are more than 10,000 nodes. Similar tendencies are observed if the maximum, standard deviation or percentiles of the irregularity distribution are compared, instead of the average. By improving the yarn boundaries representation, it is expected that the error induced in the homogenization analysis by the non-conformal approach will be mitigated, as will be confirmed in the subsequent section.

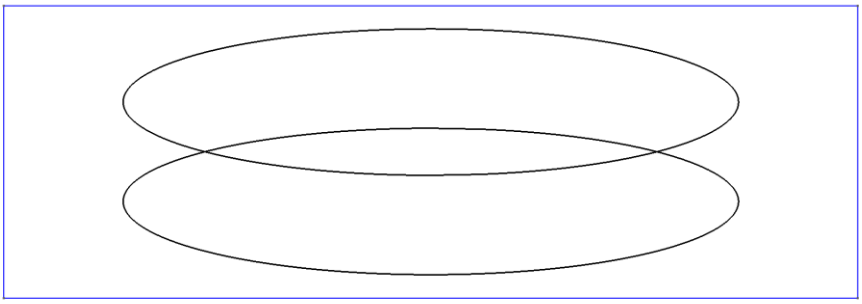

Figure 1: Example of penetrating textiles.

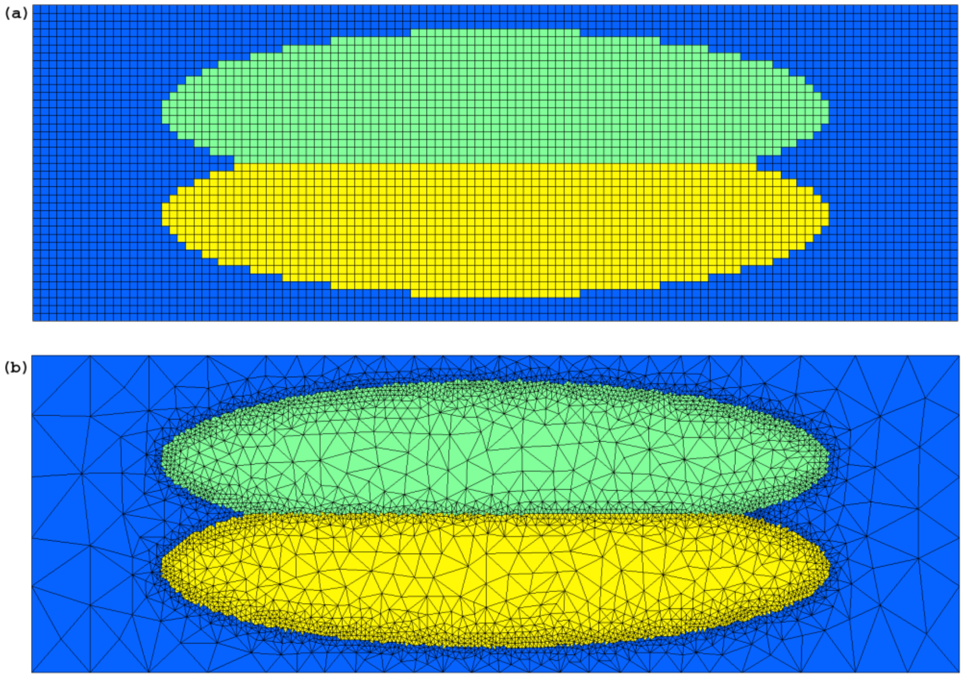

Figure 2: (a) Voxel mesh representation of the penetrated textile, (b) Unstructured mesh refined at boundaries. Both meshes are quadratic and contain the same number of nodes.

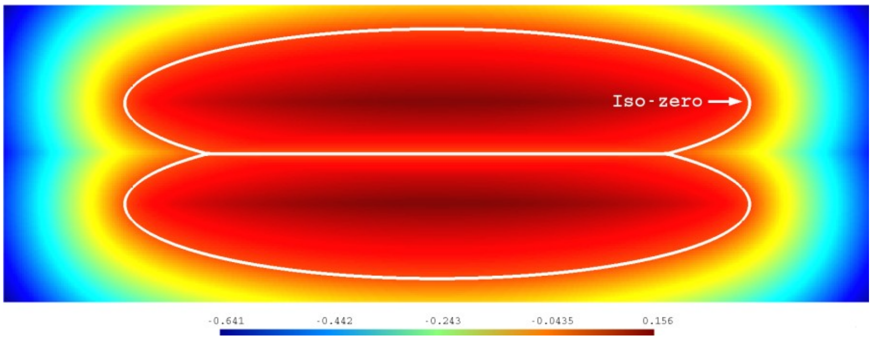

Figure 3: Computed distance field, used for mesh refinement.

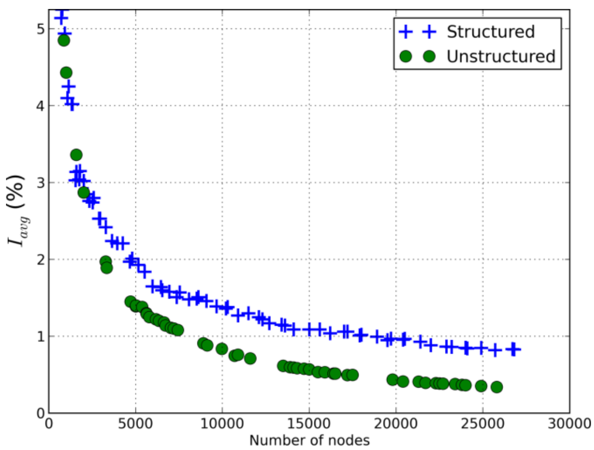

Figure 4: Interface irregularity as a function of mesh refinement.

3 FINITE ELEMENT HOMOGENIZATION

After mesh generation, the finite element method is used to determine the homogenized thermo-elastic properties of the composite, by averaging the thermo-mechanical behavior of the RVE. This approach is straightforward and has been widely used in the literature, see [6,14,28,29] for instance.

A simple plain weave textile is used to compare the unstructured meshing approach to conformal meshing and voxel meshing approaches in terms of homogenization accuracy. In order to allow for conformal meshing, a small gap is introduced between the yarns at tangency points. This gap is 0.1 % of the textile thickness and is kept the same for all meshing techniques, for the sake of consistency. A convergence study is conducted in Figure 5 to assess the accuracy of the unstructured non-conformal approach, compared to the reference conformal meshing and to voxel meshing. On these graphs, all properties are normalized by the converged value obtained with the conformal approach. The latter is very stable and does not require a very fine mesh to generate converged values, while the voxel shows very low convergence rates and low accuracy. The unstructured approach, while not perfect, provides faster convergence and a better or equal accuracy than the voxel approach for most properties. The error with respect to the conformal homogenization is less than 1 % for all properties, except for the in-plane CTE (6.2 %), with an overall average of 1.4 %. The voxel approach reached the limits of the High Performance Computing infrastructure used for the study (192 Gb of RAM) before the results could converge. This huge memory requirement for voxel meshes may be due to bad conditioning of the stiffness matrix and non-optimal settings of the FE solver. This problem is under investigation. The finest voxel mesh provided an average error of 3 %, at a much higher cost than for converged results of the unstructured approach.

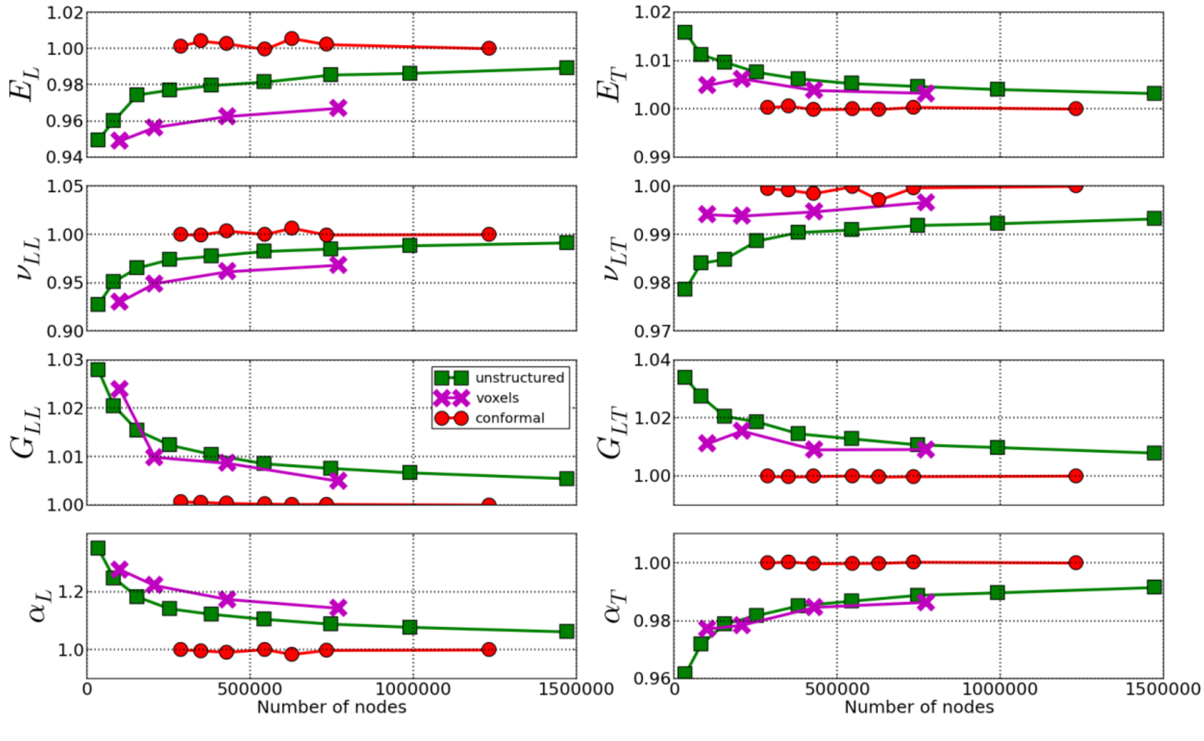

Figure 5: Convergence study with the different meshing techniques

4 COMPENSATION OF TEXTILE PENETRATIONS

The objective of the presented methodology is to produce a good approximation of the homogenized thermo-mechanical properties and microscopic stress state of complex textiles with minimum effort put into textile modeling. The resulting textile penetrations cannot be ignored in the homogenization process, mainly because they induce an artificial decrease in the yarn volume fraction, which in turn leads to a reduced fiber volume fraction.

The method is applied as follows for each yarn independently. Let us consider a given yarn. First, the yarn is cut into sections as shown in Figure 6. For each section i, the total volume of the elements which are considered to solely belong to that yarn in the FE analysis, V_{nc}^i (non-conformal volume), is computed, as well as the volume of elements which are shared with other yarns in the FE analysis V_p^i (penetration volume). The total volume of the section is hence $V_s^i = V_{nc}^i + V_p^i \geq V_{nc}^i$. This relationship implies that the meshed volume of the section is smaller than the original cross-section in the geometrical representation. This can be seen as a sort of local compaction of the fibers inside the yarn, which is taken into account by increasing locally the intra-yarn fiber volume fraction $\upsilon_{f,nc}^i$ to

$$\upsilon_{f,nc}^i = \frac{V_s^i}{V_{nc}^i} \times \frac{V_y}{V_{y,nc}} \times \upsilon_f, \tag{2}$$

where υ_f is the nominal fiber volume fraction inside the yarn, V_y is the geometrical volume of the yarn (e.g. in TexGen) and $V_{y,nc}$ is the total volume of the yarn in the non-conformal mesh, including penetrations (i.e. $V_{y,nc} = \sum_i V_s^i$). Then, the total effective fiber volume inside the yarn in the FE analysis is equal to the specification of the user in the geometrical modeler. This method emulates changes in cross-section shapes and yarn compaction in the FE representation, while keeping idealized and simple geometric modeling. After computing the local fiber volume fraction with Eq. (2), in each section of the yarn, the material properties must be determined. Considering impregnated yarns as unidirectional composites allows the use of micromechanics-based equations proposed by Chamis [30] to compute yarn material properties with fiber volume fraction $\upsilon_{f,nc}^i$. For the CTE of the yarns, micromechanics equations by Schapery [31] and Hyer [32] for the longitudinal and transverse directions, respectively, are used.

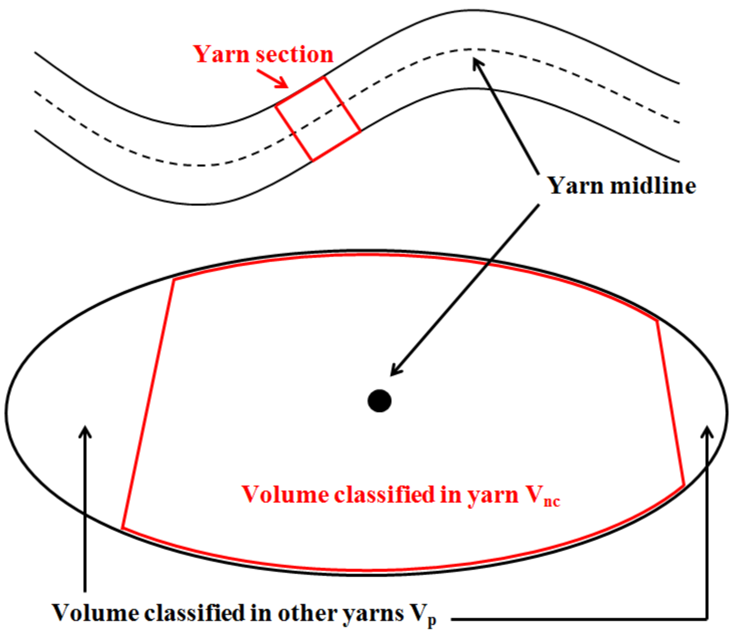

Figure 6: Yarn division and definition of penetration volumes

5 TEST CASE

A typical application of the proposed methodology is the modeling of complex, highly-compacted textiles. Stig and Hallström [6] developed a modeling framework suited to such textiles. Yarns are modeled as shells and are inflated with contact conditions in a first explicit FE analysis until a desired yarn volume fraction is reached. For the cases presented in [6], the geometrical fidelity with respect to the manufactured textile is remarkable. The yarns occupy up to 85 % of the volume of the RVE. Such compaction without yarn penetrations is out of reach with built-in functionalities of TexGen since the yarn cross-section area varies significantly both in size and shape. The simplified modeling strategy of these textiles consists in being as representative as possible as the reference textile, within the capabilities of TexGen. For instance, the simplified model is representative of the dimensions of the RVE, yarn interlacing, total yarn volume, average yarn crimp, etc. Yarn cross sections are constant, yet determined in order to reduce overall yarn penetrations.

Three textiles are reproduced from [6], referenced as S, B and D. The result of the simplified modeling for textile B is shown in Figure 7. The penetration volume, i.e. the volume that is occupied by more than one yarn, is 9.7 % of the volume of the RVE. All homogenization results are presented in Table 1. The comparison with respect to the reference finite element predictions demonstrates an average difference of 10 % for Young's moduli (6 % if the worst of the six predictions is discarded) and 10 % as well for shear moduli. However, the Poisson ratios are systematically underestimated, by 15 to 35 %. The poor correlation for the Poisson's ratios is however not that surprising since the transverse contraction is very sensitive to other model parameters. The present methodology complies very well with the experimental data presented in [6], equally well or better than the reference FE results. However, limitations were identified by the authors [6], from both experimental and modeling perspectives. The claim of the present paper is not that the new methodology is more accurate than the one developed by Stig and Hallström, but that a simplified representation of a complex textile can also provide good predictions.

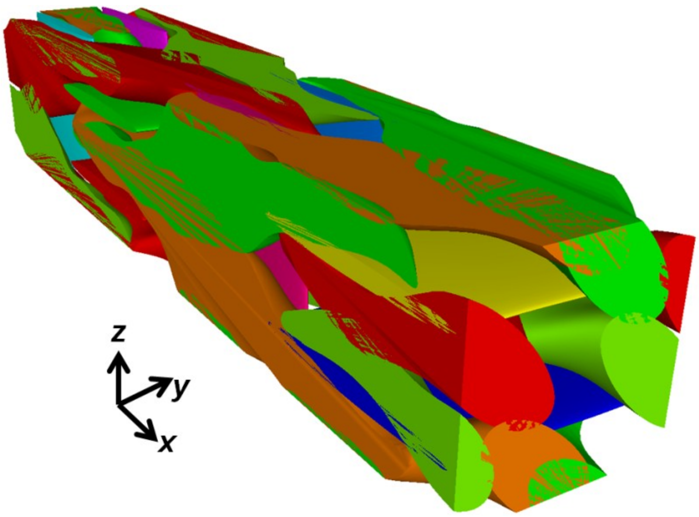

Figure 7: Simplified representation of textile B

		Textile S			Textile B			Textile D		
		FE	FE [6]	Exp. [6]	FE	FE [6]	Exp. [6]	FE	FE [6]	Exp. [6]
E_x	[GPa]	74.7	83.2	74.6 ± 0.3	59.0	65.8	58.8 ± 3.7	36.2	36.2	31.9 ± 2.1
E_y	[GPa]	11.7	12.0	–	13.3	12.5	–	15.0	11.5	–
υ_{xy}	–	0.26	0.31	–	0.27	0.36	–	0.26	0.41	–
υ_{yz}	–	0.27	0.31	–	0.23	0.28	–	0.18	0.27	–
G_{xy}	[GPa]	3.26	3.76	–	3.35	3.94	–	3.08	3.84	–
G_{yz}	[GPa]	1.93	1.93	–	1.94	1.99	–	1.95	2.19	–

Table 1: Comparison of the results from the presented method and [6].

6 CONCLUSIONS

A novel method for performing homogenization FE analysis of woven textiles regardless of yarn penetrations has been developed. It makes the best of simple textile generation features in TexGen while being as representative as possible of reference textiles modeled with more sophisticated methods. In parallel, a mesh adaptation procedure has been added to the framework for a better representation of material interfaces, and hence providing a better description of the local stress state. The overall methodology has no restrictions - from a numerical point of view - with respect to the type of textile or the amount of penetrations.

ACKNOWLEDGEMENTS

The first author is greatful to the Walloon Region (Belgium) for the financial support provided in the frame of the First DoCA OPTIMOLD project.

REFERENCES

[1] P. Vandeurzen, J. Ivens, I. Verpoest, A three-dimensional micromechanical analysis of woven-fabric composites. I. geometric analysis, *Composites Science and* T*echnology*, **56**, 1996, pp. 1303–1315.

[2] P. Vandeurzen, J. Ivens, I. Verpoest, A three-dimensional micromechanical analysis of woven-fabric composites. II. elastic analysis. *Composites Science and Technology*, 56, 1996, pp. 1317–1327.

[3] M. Paley, J. Aboudi, Micromechanical analysis of composites by the generalized cells model, *Mechanics of Materials*, **14**, 1992, pp. 127-139.

[4] B. Gommers, I. Verpoest, P. Van Houtte, The Mori-Tanaka method applied to textile composite materials, *Acta Materialia,* **46**, 1998, pp. 2223-2235.

[5] S.V. Lomov, D.S. Ivanov, I. Verpoest, M. Zako, T. Kurashiki, H. Nakai, S. Hirosawa, Meso-FE modelling of textile composites: Road map, data flow and algorithms, *Composites Science and Technology*, **67**, 2007, pp. 1870–1891.

[6] F. Stig, S. Hallström, Spatial modelling of 3D-woven textiles, *Composite Structures*, **94**, 2012, pp. 1495-1502.

[7] J.J. Crookston, S. Kari, N.A. Warrior, I.A. Jones, A.C. Long, 3D textile composite mechanical properties prediction using automated FEA of the unit cell, *Proceedings of the 16th International Conference on Composite Materials*, Kyoto, Japan, July 8–13, 2007.

[8] G. Ernst, M. Vogler, C. Hühne, R. Rolfes, Multiscale progressive failure analysis of textile composites, *Composites Science and Technology*, **70**, 2010, pp. 61-72.

[9] I. Straumit, S.V. Lomov, M. Wevers, Quantification of the internal structure and automatic generation of voxel models of textile composites from X-ray computed tomography data, *Composites: Part A*, **69**, 2015, pp. 150–158.

[10] S.D. Green, M.Y. Matveev, A.C. Long, D. Ivanov, S.R. Hallett, Mechanical modelling of 3D woven composites considering realistic unit cell geometry, *Composite Structures*, **118**, 2014, pp. 284–293.

[11] X. Zeng, L.P. Brown, A. Endruweit, M. Matveev, A.C. Long, Geometrical modelling of 3D woven reinforcements for polymer composites: Prediction of fabric permeability and composite mechanical properties, *Composites: Part A*, **56**, 2014, pp. 150–160.

[12] G. Hello, J. Schneider, Z. Aboura, Numerical simulations of woven composite materials with voxel-fe models, *Proceedings of the 16th European Conference on Composite Materials*, Seville, Spain, June 22-26, 2014.

[13] E. Potter, S.T. Pinho, P. Robinson, L. Iannucci, A.J. McMillan, Mesh generation and geometrical modelling of 3D woven composites with variable tow cross-sections, *Computational Materials Science*, **51**, 2012, pp. 103–111.

[14] H.J. Kim, C.C. Swan, Voxel-based meshing and unit-cell analysis of textile composites, *International Journal for Numerical Methods in Engineering*, **56**, 2003, pp. 977–1006.

[15] J.J. Crookston, M.N. Sherburn, L.G. Zhao, J.W. Ooi, A.C. Long, I.A. Jones, Finite element analysis of textile composite unit cells using conventional and novel techniques, *Proceedings of*

the 15th International Conference on Composite Materials, Durban, South Africa, June 27 - July 2, 2005.

[16] S.V. Lomov, I. Verpoest, J. Cichosz, C. Hahn, D.S. Ivanov, B. Verleye, Meso-level textile composites simulations: Open data exchange and scripting, *Journal of Composite Materials*, **48**, 2014, pp. 621–637, 2014.

[17] I. Verpoest, S.V. Lomov, Virtual textile composites software WiseTex: Integration with micro-mechanical, permeability and structural analysis, *Composites Science and Technology*, **65**, 2005, pp. 2563–2574.

[18] S.V. Lomov, A.V. Gusakov, G. Huysmans, A. Prodromou, I. Verpoest, Textile geometry preprocessor for meso-mechanical models of woven composites, *Composites Science and Technology*, **60**, 2000, pp. 2083-2095.

[19] L. Adam, R. Assaker, Integrated nonlinear multi-scale material modelling of fiber reinforced plastics with Digimat: application to short and continuous fiber composites, *Proceedings of the 11th World Congress on Computational Mechanics*, Barcelona, Spain, July 20-25, 2014.

[20] M.A. Melchior, M. Duflo, J.S. Gerard, L. Adam, R. Assaker, End-to-end FE based homogenization of woven composites, *Proceedings of the 14th annual SPE Automotive Composites Conference and Exhibition*, Novi, MI, USA, September 9-11, 2014.

[21] M. Sherburn, Geometric and mechanical modelling of textiles, PhD Thesis, University of Notthingham, July 2007.

[22] S.D. Green, A.C. Long, B.S.F. El Said, S.R. Hallett, Numerical modelling of 3D woven preform deformations, *Composite Structures*, **108**, 2014, pp. 747–756.

[23] Y. Mahadik, S.R. Hallett, Finite element modelling of tow geometry in 3D woven fabrics, *Composites: Part A*, **41**, pp. 1192–1200.

[24] B. Sonon, T.J. Massart, A Level-Set Based Representative Volume Element Generator and XFEM Simulations for Textile and 3D-Reinforced Composites, *Materials*, **6**, 2013, pp. 5568-5592.

[25] R.G. Rinaldi, M. Blacklock, H. Bale, M.R. Begley, B.N. Cox, Generating virtual textile composite specimens using statistical data from micro-computed tomography: 3D tow representations, *Journal of the Mechanics and Physics of Solids*, **60**, 2012, pp. 1561–1581.

[26] G. Grail, M. Hirsekorn, A. Wendling, G. Hivet, R. Hambli, Consistent Finite Element mesh generation for meso-scale modeling of textile composites with preformed and compacted reinforcements, *Composites: Part A*, **55**, 2013, pp. 143–151.

[27] Simmetrix, http://www.simmetrix.com, Simmetrix Inc., 10 Halfmoon Executive Park Drive, Clifton Park, NY 12065, USA.

[28] A.R. Labanieh, X. Legrand, V. Koncar, D. Soulat, Evaluation of the elastic behavior of multiaxis 3D-woven preforms by numerical approach, *Journal of Composite Materials*, **48**, 2013, pp. 3243-3252.

[29] X.F. Wang, X.W. Wang, G.M. Zhou, C.W. Zhou, Multi-scale Analyses of 3D Woven Composite Based On Periodicity Boundary Conditions, *Journal of Composite Materials*, **41**, 2007, pp. 1773-1788.

[30] C.C. Chamis, Simplified composite micromechanics equations for strength, fracture toughness and enviromental effects, SAMPE Quart, 1984.

[31] R.A. Schapery, Thermal expansion coefficients of composite materials based on energy principles, *Journal of Composite Materials*, **2**, 1968, pp. 380-404.

[32] M.W. Hyer, Stress analysis of fiber-reinforced materials, 2nd edn. Lancaster, PA : Destech Publications, Inc., 2009.